Chemico-Biological Interactions 207 (2014) 16–22

Contents lists available at ScienceDirect

Chemico-Biological Interactions

journal homepage: www.elsevier.com/locate/chembioint

A bufadienolide derived androgen receptor antagonist with inhibitory activities against prostate cancer cells

Hai-Yan Tian [a,1], Xiao-Feng Yuan [a,1], Lu Jin [a,1], Juan Li [a], Cheng Luo [b], Wen-Cai Ye [a,*], Ren-Wang Jiang [a,*]

[a] Institute of Traditional Chinese Medicine and Natural Products, College of Pharmacy, Jinan University, Guangzhou 510632, PR China
[b] State Key Laboratory of Drug Research, Shanghai Institute of Materia Medica, Chinese Academy of Sciences, 555 Zu Chong Zhi Road, Shanghai 201203, PR China

ARTICLE INFO

Article history:
Received 8 September 2012
Received in revised form 4 October 2013
Accepted 24 October 2013
Available online 5 November 2013

Keywords:
Androgen receptor
Antagonist
Bufadienolide
Molecular docking
Na^+/K^+ ATPase

ABSTRACT

Molecular docking studies have shown that $\Delta^{8,14}$-anhydrobufalin (**1**) exhibited more potent binding affinity on androgen receptor (AR) than $\Delta^{14,15}$-anhydrobufalin (**2**) and bufalin (**3**). To validate the docking results, compounds **1** and **2** were synthesized. The AR competitive binding assay indicated that the IC_{50} values of **1**–**3** were 1.9, >50 and >50 μM (relative binding affinity), respectively, which confirmed that our theoretical binding mode was reliable and predictable. Furthermore, compound **1** was found to show more potent inhibitory activity against the androgen dependent LNCaP cancer cells than the androgen independent PC3 cancer cells, but exhibited less inhibition on the Na^+/K^+ ATPase as compared with the parent compound **3**. To the best of our knowledge, compound **1** represented the first AR antagonist derived from bufadienolide discovered through a series of combined approaches of molecular docking and actual experimental validation.

1. Introduction

Androgen receptor (AR) belongs to the steroid nuclear receptor super-family [1]. It is activated by endogenous androgens as testosterone and 5a-dihydrotestosterone (DHT) or exogenous compounds, and regulates genes for male differentiation and development [2]. However, high levels of AR expression may lead to severe diseases like prostate cancer (PCa). Recently, AR was found to play a critical role in PCa since approximately 80–90% of PCa are androgen dependent at initial diagnosis [3,4]. Thus it has become an attractive target for the treatment of PCa. Although several pure AR antagonists, such as bicalutamide and flutamide, were developed for PCa therapy, they could not completely blocks binding of DHT to AR and the small amount of free DHT still stimulate prostate cancer growth [5]. Furthermore, bicalutamide can exhibit some agonist activity in cells containing mutant AR [6]. Thus, a sustained effort for the development of new and more effective AR antagonist has been undertaken.

Bufalin (**3**, Scheme 1), a typical bufadienolide, has been reported to show potent antineoplastic activity against human prostate cancer cells LNCaP and DU145 [7]. However, it was reported to be five times more lethal than ouabain due to its much stronger inhibition on Na^+/K^+-ATPase [8], which greatly hindered the clinical application [9].

Close examination of the structure of **3** revealed the similarity to those of steroidal AR antagonists, such as VN/85-1 [10]. Both of them possessed a steroidal skeleton with an unsaturated substitution at C-17. However, the steroid moiety of bufalin is saturated in contrast to the presence of at least one double bond in the steroidal AR antagonists. We hypothesized that introduction of a double bond in bufalin would increase the interactions with androgen receptor.

In order to test the hypothesis, firstly, we virtually introduced a double bond around the hydroxyl group at C-14 of **3** considering that it was in the middle of the molecule and important for the conformation of the whole molecule. Then, the molecular docking method was used to compare the interactions of **3** and the two derivatives, i.e., $\Delta^{8,14}$-anhydrobufalin (**1**) and $\Delta^{14,15}$-anhydrobufalin (**2**, Scheme 1) with androgen receptor. Finally, the actual derivatives were synthesized and their activities toward the two molecular targets were tested.

2. Materials and methods

2.1. Molecular docking study of compounds 1–3 to AR

2.1.1. Homology modeling

The 3D model of the androgen receptor (AR) in its inactive form was constructed based on the known antagonist form of human glucocorticoid receptor (PDB ID: 3H52) [11], a homologous protein

* Corresponding authors. Tel./fax: +86 20 85221559.
E-mail addresses: chyewc@gmail.com (W.-C. Ye), trwjiang@jnu.edu.cn, rwjiang2008@126.com (R.-W. Jiang).
[1] These authors contribute equally to this work.

0009-2797/$ - see front matter © 2013 Elsevier Ireland Ltd. All rights reserved.
http://dx.doi.org/10.1016/j.cbi.2013.10.020

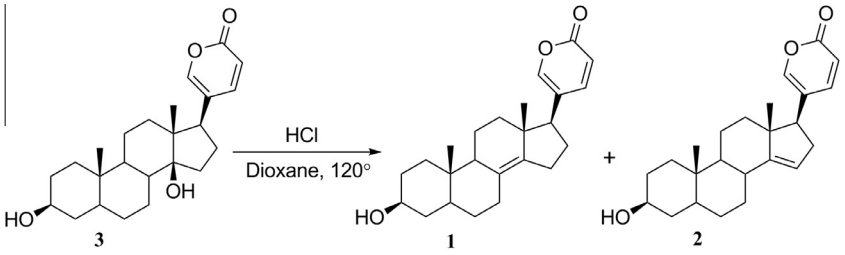

Scheme 1. Structure formulae of compounds **1**–**3**.

of AR (they share >50% sequence similarity) and an agonist form of AR (PDB ID: 2PIT) [12]. Sequence alignment and homology modeling were performed using Modeller V9.10 [13]. The final sequence alignment was visualized using ESpript [14] as shown in Fig. 1.

2.1.2. Molecular dynamic (MD) simulation

In order to obtain a more stable conformation of AR in solution, MD simulation was performed. Simulations were conducted with the OPLS all-atom force-field implemented in GROMACS 4.5.3 [15]. Topology files were generated using pdb2gmx module in Gromacs, then this system was solvated by water suing TIP4P water model in a cubic box extending 10 Å around the receptor. In addition, the system was neutralized using sodium chloride and the concentration was adjusted to 0.17 mM by genion (in Gromacs). Long-range electrostatic interactions were treated using the particle-mesh Ewald method [16]. Periodic boundary conditions were applied to avoid edge effects in all calculations. The temperature was kept constant at 300 K by separately coupling the water, ions, and protein in a thermal bath using the Berendsen thermostat method [17] with a coupling time of 2 ps. Berendsen pressure coupling was used for the equilibration of the systems. The solvated system was underwent two energy minimizations with protein position constrained and none restrain at all. Following, energy minimized solvated system was equilibrated by 100 ps protein position restrained NVT and NPT process at 300 K. Finally, a 10 ns NPT equilibration was conducted without restriction. After 10 ns equilibration, the final conformation was extracted and used for docking.

2.1.3. Molecular docking

2.1.3.1. Protein preparation and grid generation. Protein structure was prepared with Protein Preparation Wizard [18] in Maestro 9.0, energy was minimized using OPLS force-field and default setting. The A chain of antagonist human glucocorticoid receptor was overlapped into above mentioned structure, and the position of co-crystallized ligand was used as a reference for next step. Grid was generated by Glide 5.5 using default setting.

2.1.3.2. Ligand preparation. Ligand was drawn using Maestro 9.0 [19] and prepared using LigPrep [20] application. MMFFs force-field was chosen. Other parameters use default values.

2.1.3.3. Docking procedure. Molecular docking was performed using Induced Fit Docking (IFD) [21] and Rigid Docking [22] modules in Maestro 9.0 (SP mode). The ligand flexibility was considered in both approaches. Grid box was centered on R752, R711, L704 and W741, which was based on crystal structure of AR bound to DTH (PDB ID: 2PIT) [12]. Since the binding site of AR is a very large binding cavity, we extend the outer box length to 24.6 Å (from 18.7 Å). Flexible residues were defined using residues within 5.0 Å distance from the reference ligand for the Induced Fit Docking method, while for the Rigid Docking method, all residues were kept rigid. Best pose of each molecule was extracted, and final result was visualized using PyMol 1.3 [23] and LigPlot [24].

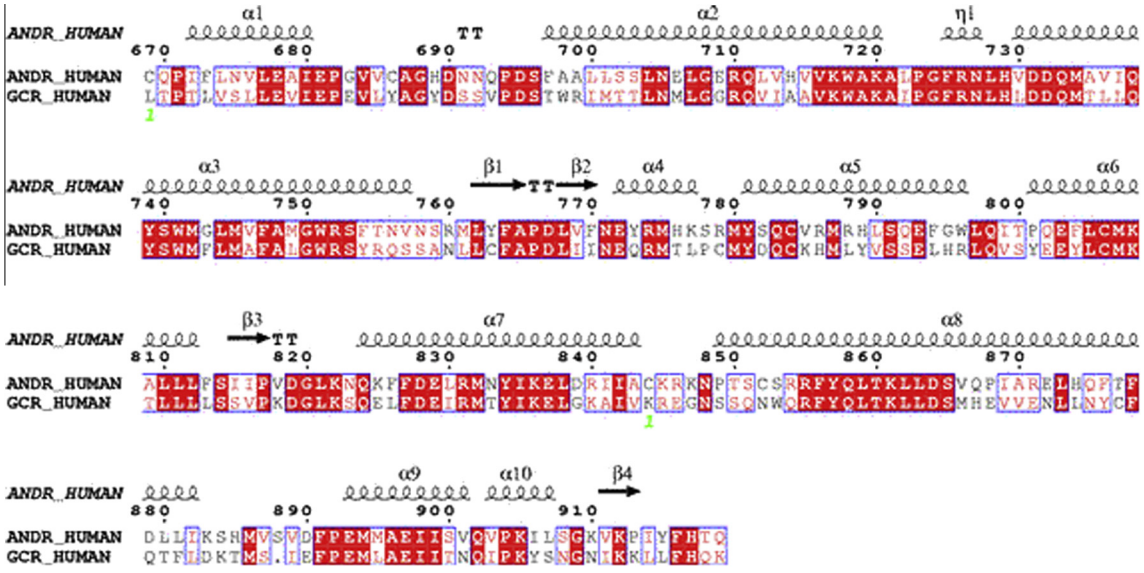

Fig. 1. Sequence alignment was performed in Modeller 9.10 and drawn with ESPript. The sequence of androgen receptor (PDB code: 2PIT) was shown on the upper side and the sequence of glucocorticoid receptor (PDB code: 3H52) was shown downside.

2.2. Chemistry

2.2.1. General methods

ESI-MS spectra were carried out on a Finnigan LCQ Advantage Max ion trap mass spectrometer. HR-ESI-MS data were obtained on an Agilent 6210 ESI/TOF mass spectrometer. NMR spectra were measured on Bruker AV-400 spectrometer. The solvents used in column chromatography and HPLC were of analytical grade (Shanghai Chemical Plant, Shanghai, P.R. China) and chromatographic grade (Fisher Scientific, New Jersey, U.S.A.), respectively.

2.2.2. Synthesis of bufalin derivatives **1** and **2**

To a solution of bufalin (50 mg) dissolved in 10 ml of dioxane, 35% hydrochloric acid solution (500 μl) was added, which was sealed and then heated at 120 °C in an oil bath with a magnetic stirrer for 4 h. The solution was neutralized with 27% ammonia water, and evaporated under reduced pressure to give a residue, which was subsequently partitioned between water and $CHCl_3$. The $CHCl_3$ fraction was separated using preparative HPLC using acetonitrile–water (60:40) as the mobile phase to give **1** (20.8 mg, 48.4%) and **2** (3.0 mg, 6.9%).

$\Delta^{8,14}$-Anhydrobufalin (**1**): Colorless crystals, ^{1}H NMR ($CDCl_3$, 400 MHz) δ = 1.47 (2H, m, H-1), 1.57 (2H, m, H-2), 4.02 (1H, br s, H-3), 1.39 (1H, m, H-4α), 2.08 (1H, m, H-4β), 1.82 (1H, m, H-5), 1.23 (1H, m, H-6α), 1.87 (1H, m, H-6β), 2.36 (1H, m, H-7α), 1.88 (1H, m, H-7β), 2.40 (1H, m, H-9), 1.54 (1H, m, H-11α), 1.45 (1H, m, H-11β), 1.15 (1H, m, H-12α), 1.61 (1H, m, H-12β), 1.88 (1H, m, H-15α), 2.36 (1H, m, H-15β), 1.88 (1H, m, H-16α), 2.18 (1H, m, H-16β), 2.24 (1H, dd, J = 12.6, 6.9 Hz, H-17), 0.71 (3H, s, H-18), 0.83 (3H, s, H-19), 7.27 (1H, br s, H-21), 7.30 (1H, dd, J = 9.5, 2.6 Hz, H-22), 6.29 (1H, br d, J = 9.5 Hz, H-23) ppm; ^{13}C NMR ($CDCl_3$, 100 MHz) δ = 29.4 (C-1), 28.3 (C-2), 67.0 (C-3), 33.2 (C-4), 36.6 (C-5), 26.8 (C-6), 25.3 (C-7), 129.3 (C-8), 35.7 (C-9), 37.0 (C-10), 19.5 (C-11), 43.4 (C-12), 49.5 (C-13), 138.6 (C-14), 25.3 (C-15), 24.7 (C-16), 51.8 (C-17), 18.7 (C-18), 24.1 (C-19), 118.4 (C-20), 148.8 (C-21), 145.3 (C-22), 115.4 (C-23), 162.1 (C-24) ppm.

$\Delta^{14,15}$-Anhydrobufalin (**2**): Colorless crystals, ^{1}H NMR (CD_3OD, 400 MHz) δ = 4.02 (1H, br s, H-3), 5.28 (1H, m, H-15), 2.82 (1H, dd, J = 10.6, 8.2 Hz, H-17), 0.75 (3H, s, H-18), 0.96 (3H, s, H-19), 7.54 (1H, br s, H-21), 7.58 (1H, dd, J = 9.6, 2.6 Hz, H-22), 6.32 (1H, br d, J = 9.6 Hz, H-23); ^{13}C NMR (CD_3OD, 100 MHz) δ = 30.8 (C-1), 28.6 (C-2), 67.7 (C-3), 34.2 (C-4), 36.4 (C-5), 25.1 (C-6), 27.5 (C-7), 36.7 (C-8), 41.2 (C-9), 37.8 (C-10), 22.8 (C-11), 42.2 (C-12), 49.5 (C-13), 155.5 (C-14), 117.9 (C-15), 34.5 (C-16), 54.1 (C-17), 19.3 (C-18), 24.1 (C-19), 120.9 (C-20), 150.6 (C-21), 147.9 (C-22), 115.8 (C-23), 164.6 (C-24).

2.2.3. X-ray crystallographic analyses of compound **1** and **2**

Colorless crystals of both compounds **1** and **2** were obtained via slow evaporation of a methanol solution. Data collections were performed on an Agilent Gemini S Ultra CCD diffractometer. The crystal structures were solved by direct methods using SHELXS-97 and refined by full-matrix least-squares method on F^2 using SHELXTL v.510. Non-hydrogen atoms were subjected to anisotropic refinement. Hydrogen atoms bonded to carbons were placed at their idealized positions with assigned isotropic thermal parameters and included in the calculation of structure factors.

Compound **1**, $C_{24}H_{32}O_3{\cdot}H_2O$, M = 386.51, Orthorhombic, space group P2(1)2(1)2(1), a = 7.50080(10), b = 10.4630(2), c = 26.5100(4)Å, V = 2080.53(6)Å^3, Z = 4, D_c = 1.279 Mg/m^3, F(000) = 840, μ(Cu-Kα) = 0.653 mm^{-1}, $3.33 \leqslant \theta \leqslant 62.67$, unique reflections = 2867, R = 0.0439, S = 1.055, CCDC No. 898322.

Compound **2**, $C_{24}H_{32}O_3$, M = 368.50, Orthorhombic, space group P2(1)2(1)2(1), a = 8.46030(10), b = 12.7309(2), c = 19.1062(3)Å, V = 2057.88(5)Å^3, Z = 4, D_c = 1.189 Mg/m^3, F(000) = 800, μ(Cu-Kα) = 0.601 mm^{-1}, $4.17 \leqslant \theta \leqslant 62.57$, unique reflections = 3230, R = 0.0580, S = 1.038, CCDC No. 898321.

2.3. AR competitive binding assay

The fluorescence polarization (FP) technique was used to determine the binding affinity of compounds **1**–**3** using PolarScreenTM Androgen Receptor Competitor Assays kit (Catalog # P3018) purchased from Invitrogen [25]. Essentially, the protocol involved titration of different concentration of competitive ligand against the pre-formed complex of Fluormone AL green (2 nM) and the AR-LBD (50 nM). The assay mixture was allowed to equilibrate at 20–25 °C in 384-well plates for 4 h, after which the polarization values are measured at room temperature using the Perkin Elmer EnVision Multilabel Reader. The excitation and emission wavelength values for the Fluormone were 480 and 535 nM, respectively. The data analysis for the ligand binding assays was done using GraphPad Prism 5 software. The IC_{50} values were calculated by the equation:

$$Y = \mathrm{mP}_{100\%} + (\mathrm{mP}_{0\%} - \mathrm{mP}_{100\%})/1 + 10((\mathrm{LogIC}_{50} - X) \times \mathrm{Hillslope}),$$

where: Y = mP, X = Log [inhibitor], $\mathrm{mP}_{100\%}$ = 100% inhibition, and $\mathrm{mP}_{0\%}$ = 0% inhibition [25].

2.4. Inhibition of Na^+/K^+-ATPase activity

The Na^+/K^+ ATPase inhibitory activities of these derivatives were determined according to the reported method [26].

2.5. Cytotoxicity of 1 against prostate cancer cells

The MTT [3-(4,5-dimethylthiazol-2-yl)-2,5-diphenyltetrazolium bromide] assay was done as described previously [27] with taxol served as the positive control. Briefly, 3×10^3 cells per well for PC3 cell line and 5×10^3 cells per well for LNCaP cell line were plated into the 96-well plates, respectively and placed in the incubator overnight using the standard culture conditions as reported [28]. A series diluted compound **1** was added to each well. After 48 h of exposure, the cells were stained with MTT. Cell growth (viability) was determined by measuring optical density at 570 nM with a microplate reader (TECAN Spectra II Plate Reader, Research Triangle Park, N.C.). The relative cell growth (%) was expressed as a percentage relative to the untreated control cells. The experiments were repeated twice, each in triplicate.

3. Results and discussion

Androgens and anti-androgens bind to the Ligand binding domain (LBD) of AR in different manners. The former (e.g. DHT or R1881) serves as agonists, and the binding is often accompanied by activation of associated gene expression and many other related biological responses [29,30]. In contrast, the latter serves as antagonists, and the binding often induces a conformational change of AR LBD and leads to impairment or loss of functions [31].

$\Delta^{8,14}$-Anhydrobufalin (**1**) and $\Delta^{14,15}$-anhydrobufalin (**2**) were virtually modified from **3** through dehydration around the hydroxyl group at C-14. Because of the similar structures of **1**–**2** with those of AR antagonists, e.g. VN/85-1 [10] and abiraterone [32], we inferred that **1**–**2** might target the AR as antagonists. Thus a three-dimensional structure describing the inactive conformation of AR LBD was required. However, currently, the crystal structure of steroidal antagonist-AR LBD was not available. So a homology model of antagonist complex AR was constructed based on the known agonist complex of androgen receptor and antagonist

complex of human glucocorticoid receptor which was a close related hormone receptor.

In order to refine our initial model and obtain a more stable structure in the solvated environment, a 10 ns molecular dynamics simulation was performed [33,34]. The relative structural drift was measured by recording the RMSD of all heavy atoms versus the simulation time. It was found that the protein structure drifted rapidly from the initial structure within the first 1 ns, and still fluctuated until 4.2 ns (Fig. S1). Then the RMSD value stabilized around 1.5 Å, indicating that the structure was relatively stable and 10 ns simulation was sufficient for stabilizing a fully relaxed model. Superimposing the refined structure with initial structure, we found that the H12 Helix was most flexible which was consistent with the literature [35] and other characteristic substructures, such as H3, H7 and H10 helix were relatively stable during the simulation (Fig. S2). The average RMSD value between two structures reads 1.43 Å. Considering the improved stability and similarity to the initial structure, the structure acquired from MD simulation was used for docking experiments.

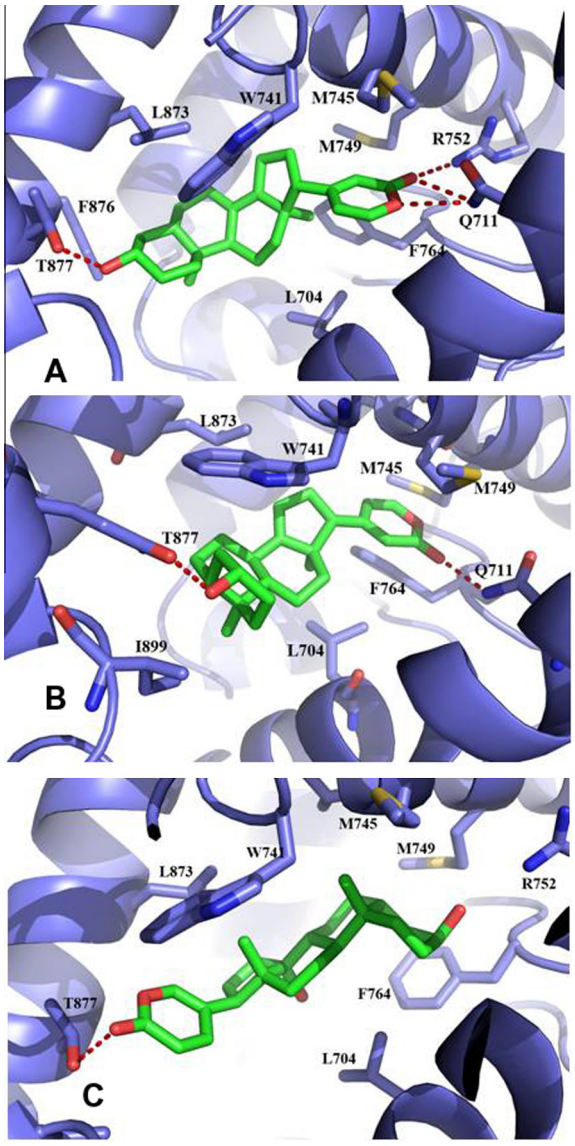

Fig. 2. Binding mode of compounds **1** (A), **2** (B) and **3** (C) in AR: dashed lines represent hydrogen bonds.

Bufalin (**3**) and its unsaturated derivatives, $\Delta^{8,14}$-anhydrobufalin (**1**) and $\Delta^{14,15}$-anhydrobufalin (**2**) were subsequently docked into the LBD of the modeled AR (Fig. 2) using an Induced Fit Docking methods. Compounds **1**–**3** adopted obvious different poses when penetrated into the binding pocket. In the complex of compound **1** with AR, the lactone ring was close to Arg 752 (R 752) and Gln 711 (Q 711), generating a bifurcated H-bond from 24-carbonyl group to both of the two amino acid residues. Besides, the hydroxyl group at C-3 served as a hydrogen donor to form the third hydrogen bond with Thr 877 (T877), which was believed to play a role in both ligand binding and receptor activation [36]. Compound **2** was in the same direction as **1** when inserted into the pocket, but the hydrogen bond with Arg 752 was lost. In contrast, compound **3** took an absolutely opposite gesture in the AR pocket. The carbonyl group at C-24 was near to Thr 877 (T 877), but no hydrogen bond was formed between the hydroxyl group at C-3 of the ligand and the receptor. Furthermore, close examination of the ligand conformations in the bound conformations obtained by docking revealed that compound **1** was more bended to form an arched shape than the other two compounds, which is favorable for the AR LBD. It was observed that **1** was more tightly wrapped up by a hydrophobic pocket composed of I899, M780, F764, L704, M745, M749, V746, L873, W741 and F876, thereby increasing the hydrophobic contacts with the LBD (Fig. 3). In addition, we also used the rigid docking method to compare the binding patterns of **1**–**3** with AR, which showed the same tendency for those compounds as the Induced Fit Docking method (Table S1, Supporting information). The binding poses of **1** obtained from rigid and flexible docking also share similar binding pattern (Fig. S3, Supporting information). However, it is noteworthy that the flexible docking protocol did improve the prediction theoretical binding affinity (for example, the 3-OH in the ligand formed hydrogen bond with T877 of AR). These above results suggested **1** could be a potential inhibitor of androgen receptor.

In order to validate the results of molecular docking, we initiated an experiment to synthesize the derivatives **1** and **2**. A dioxane solution of bufalin was heated under an acid condition (HCl) to yield two major peaks, which were subsequently separated by preparative HPLC (Fig. 4). The structures of the two peaks were elucidated to be $\Delta^{8,14}$-anhydrobufalin (**1**) and $\Delta^{14,15}$-anhydrobufalin (**2**) based on their HR-ESI-MS and NMR data. The structures of these two compounds were reported before [37]; however, only ^{1}H NMR data was available and the stereochemistry was unknown. In the present study, the full assignments of the NMR data of **1** and **2** were achieved by extensive 1D and 2D NMR analysis. Furthermore, the complete structure and stereochemistry of **1** and **2** were confirmed by single-crystal X-ray analysis (Fig. 5).

The relative affinity of compounds **1**, **2** and **3** on AR were evaluated by a Polar Screen Androgen Receptor Competitor Assay Kit [25]. Compound **1** showed the highest relative affinity with the IC_{50} value of 1.9 μM, which was comparable to the positive control (progesterone IC_{50} value of 2.40 μM), indicating that it competed with the high affinity AR ligand (Fluormone™ AL Green). In contrast, compounds **2** and **3** were nearly inactive on AR with IC_{50} value larger than 50 μM. The dose-dependent curves for **1**–**3** were shown in Fig. 6. The relative binding affinities of **1**–**3** were consistent with the geometrical complementarities and stabilizing interactions in the binding pose as predicted by molecular docking analysis. It is noteworthy that though experimental IC_{50} values indicated a much higher relative binding affinity for compound **1** than for **2** and **3**, the docking scores (Table S1, supporting information) did not differentiate the relative affinity of the three compounds very much, which confirmed that the scoring functions of the docking programs might not make a definite prediction of ligand's relative binding affinity [38].

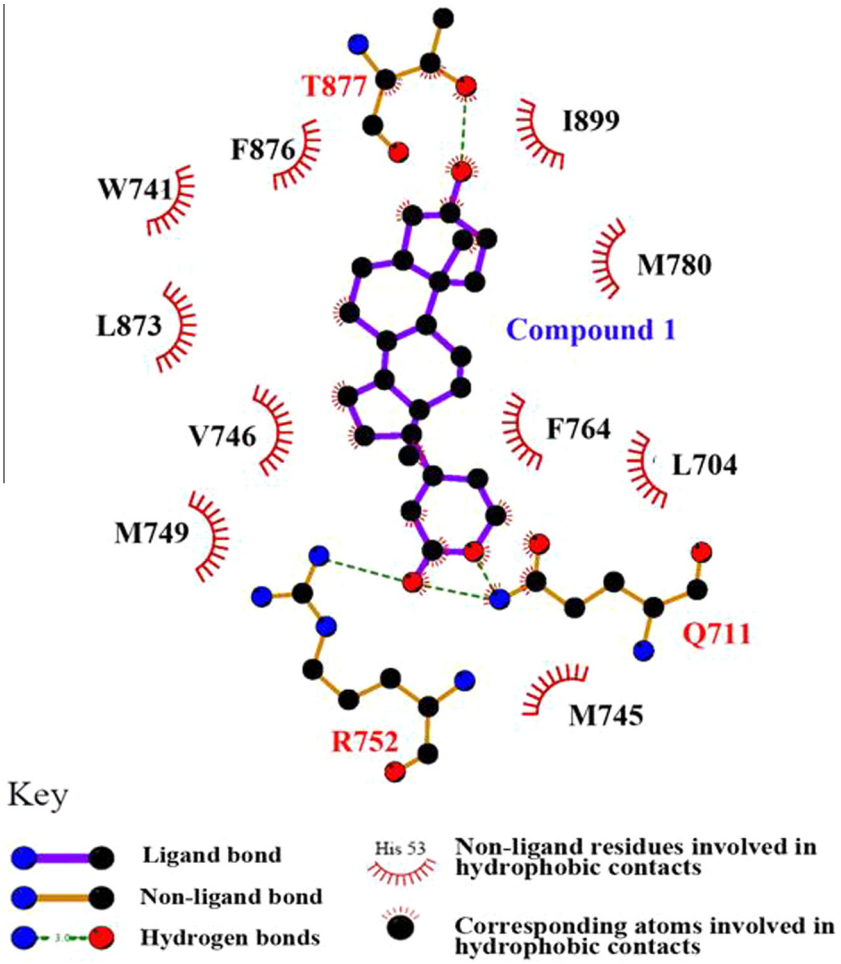

Fig. 3. Hydrophobic interactions of compound **1** with AR.

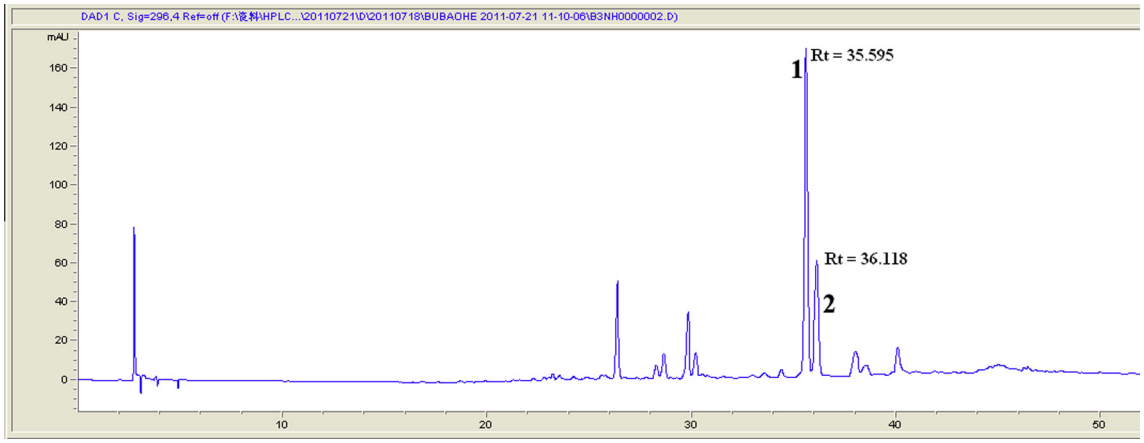

Fig. 4. HPLC chromatogram of bufalin derivatives **1** and **2**.

The active **1** was further tested for the cytotoxic activities on the androgen dependent prostate cancer cells LNCaP and androgen independent cells PC3 with taxol served as the positive control. It was found that **1** showed more potent inhibitory activity against LNCaP cells with an IC_{50} value of 6.8 μM than PC3 cells with an IC_{50} value of 16.4 μM. The dose-dependent curves of compound **1** on cell growth was shown in Fig. 7.

The inhibitory activity of **1** on Na^+/K^+ ATPase was also explored. It was found that **1** showed much weaker inhibition with an IC_{50} value of 5.6 μM than bufalin (**3**, IC_{50} value of 0.022 μM), indicating two hundred fold decrease of inhibition on Na^+/K^+ ATPase.

In summary, the unsaturated derivatives of bufalin were virtually constructed and docked into the ligand binding domain of AR using an flexible method (both the ligand and receptor were treated flexible), which suggested that the derivative **1** with a double bond between C8 and C14 showed strong hydrogen bonding and hydrophobic interactions with AR. Subsequently, the active derivative was synthesized and the relative AR binding activity

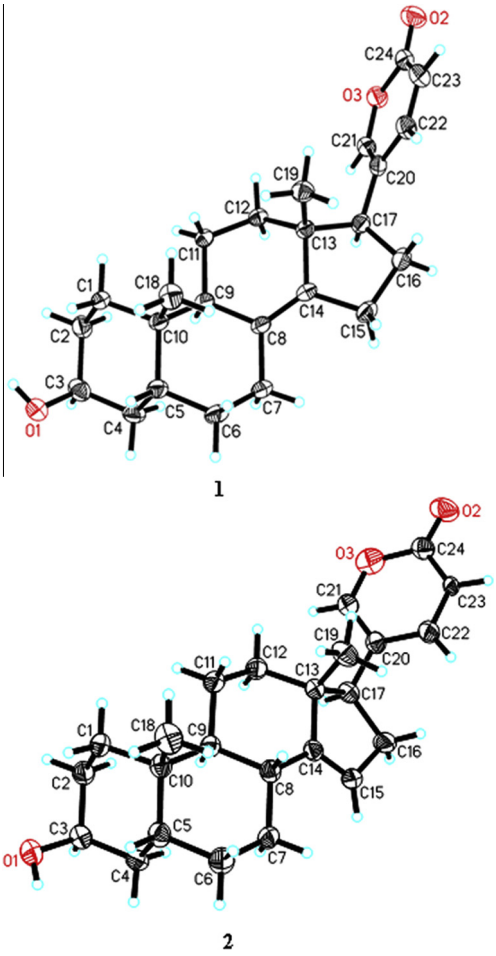

Fig. 5. Crystal structures of compounds **1** and **2**.

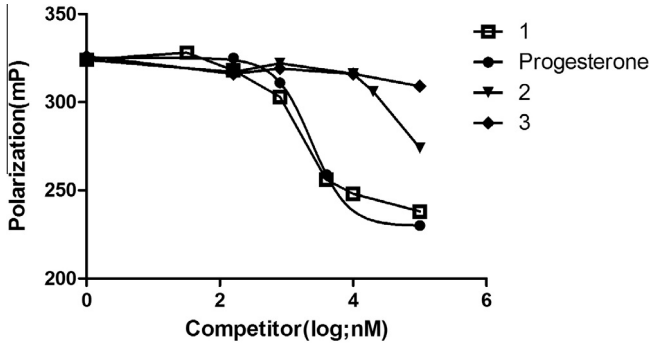

Fig. 6. The competition binding curves for compounds **1**–**3**. The protocol involved titration of different concentration of compounds **1**–**3** against the pre-formed complex of Fluormone AL green (2 nM) and the AR-LBD (50 nM). The assay mixture was allowed to equilibrate at 20–25 °C in 384-well plates for 4 h, after which the polarization values are measured at room temperature using the Perkin Elmer EnVision Multilabel Reader.

was tested by a Polar Screen Androgen Receptor Competitor Assay. Compound **1** was found to show more potent inhibitory activity against the androgen dependent LNCaP cells than the androgen independent PC3 cells. Furthermore, it showed less inhibitory effect on the Na^+/K^+-ATPase as compared with the parent compound **3**. Our results suggested that compound **1** might serve as a promising chemopreventive agent against prostate cancer. Though a large number of androgen receptor antagonists were reported [39,40], to the best of our knowledge, it is the first time to discover

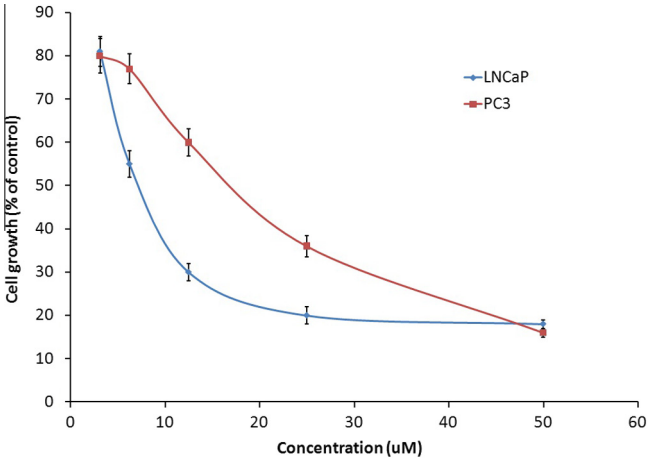

Fig. 7. The dose response curve of compound **1** by plotting the cell growth vs series concentrations. PC3 cancer cells (3×10^3 cells per well) and LNCaP cancer cells (5×10^3 cells per well) were plated into the 96-well plates, respectively and placed in the incubator overnight. A series diluted compound **1** was added to each well. After 48 h of exposure, the cells were stained with MTT. The relative cell growth (%) was determined by measuring optical density at 570 nM with a microplate reader, and was expressed as a percentage relative to the untreated control cells.

a cardiac steroid-like antagonist through combined approaches of molecular docking and validation by chemical synthesis and bioassays. Further work is warranted to investigate compound **1**'s effects on AR-mediated functional gene expression.

Conflict of interest

None declared.

Acknowledgements

This work is dedicated to Professor James Trotter in celebration of his 80th birthday, and was financially supported by the Guangdong High Level Talent Scheme to R.W.J., the Fundamental Research Funds for the Central Universities (11612603), National Natural Science Foundation of China (81102518), and Postdoctoral Granted Financial Support (20110490915).

Appendix A. Supplementary data

Supplementary data associated with this article can be found, in the online version, at http://dx.doi.org/10.1016/j.cbi.2013.10.020.

References

[1] P.M. Matias, P. Donner, R. Coelho, M. Thomaz, C. Peixoto, S. Macedo, N. Otto, S. Joschko, P. Scholz, A. Wegg, S. Bäsler, M. Schäfer, U. Egner, M.A. Carrondo, Structural evidence for ligand specificity in the binding domain of the human androgen receptor, J. Biol. Chem. 275 (2000) 26164–26171.
[2] M.A. Fousteris, U. Schubert, D. Roell, J. Roediger, N. Bailis, S.S. Nikolaropoulos, A. Baniahmad, A. Giannis, 20-Aminosteroids as a novel class of selective and complete androgen receptor antagonists and inhibitors of prostate cancer cell growth, Bioorg. Med. Chem. 18 (2010) 6960–6969.
[3] J.D. Joseph, B.M. Wittmann, M.A. Dwyer, H.X. Cui, D.A. Dye, D.P. McDonnell, J.D. Norris, Inhibition of prostate cancer cell growth by second-site androgen receptor antagonists, Proc. Natl. Acad. Sci. USA 106 (2009) 12178–12183.
[4] L. Gao, J. Alumkal, MDV-3100 androgen receptor antagonist prostate cancer therapy, Drugs Future 36 (2011) 371–376.
[5] S. Gauthier, C. Martel, F. Labrie, Steroid derivatives as pure antagonists of the androgen receptor, J. Steroid Biochem. Mol. Biol. 132 (2012) 93–104.
[6] C.D. Chen, D.S. Welsbie, C. Tran, S.H. Baek, R. Chen, R. Vessella, M.G. Rosenfeld, C.L. Sawyers, Molecular determinants of resistance to antiandrogen therapy, Nat. Med. 10 (2004) 33–39.

[7] C.H. Yu, S.F. Kan, H.F. Pu, E.J. Chien, P.S. Wang, Apoptotic signaling in bufalin- and cinobufagin-treated androgen-dependent and -independent human prostate cancer cells, Cancer Sci. 99 (2008) 2467–2476.
[8] R.J. Bick, B.J. Poindexter, R.R. Sweney, A. Dasgupta, Effects of Chan Su, a traditional Chinese medicine, on the calcium transients of isolated cardiomyocytes: cardiotoxicity due to more than Na^+, K^+-ATPase blocking, Life Sci. 72 (2002) 699–709.
[9] F.B. Jr, B.M. Kirrane, B.W. Cotter, R.S. Hoffman, L.S. Nelson, Cardioactive steroid poisoning: a comparison of plant- and animal-derived compounds, J. Med. Toxicol. 2 (2006) 152–155.
[10] S.M. Singh, S. Gauthier, F. Labrie, Androgen receptor antagonists (antiandrogens): structure–activity relationships, Curr. Med. Chem. 7 (2000) 211–247.
[11] G.A. Schoch, B. D'Arcy, M. Stihle, D. Burger, D. Bär, J. Benz, R. Thoma, A. Ruf, Molecular switch in the glucocorticoid receptor: active and passive antagonist conformations, J. Mol. Biol. 395 (2010) 568–577.
[12] E. Estébanez-Perpiñá, L.A. Arnold, P. Nguyen, E.D. Rodrigues, E. Mar, R. Bateman, P. Pallai, K.M. Shokat, J.D. Baxter, R.K. Guy, P. Webb, R.J. Fletterick, A surface on the androgen receptor that allosterically regulates coactivator binding, Proc. Natl. Acad. Sci. USA 104 (2007) 16074–16079.
[13] A. Sali, T.L. Blundell, Comparative protein modelling by satisfaction of spatial restraints, J. Mol. Biol. 234 (1993) 779–815.
[14] P. Gouet, X. Robert, E. Courcelle, ESPript/ENDscript: extracting and rendering sequence and 3D information from atomic structures of proteins, Nucleic Acids Res. 31 (2003) 3320–3323.
[15] D. Van Der Spoel, E. Lindahl, B. Hess, G. Groenhof, A.E. Mark, H.J. Berendsen, GROMACS: fast, flexible, and free, J. Comput. Chem. 26 (2005) 1701–1718.
[16] U. Essmann, L. Perera, M.L. Berkowitz, T. Darden, H. Lee, L.G. Pedersen, A smooth particle mesh Ewald method, J. Chem. Phys. 103 (1995) 8577–8593.
[17] H.J.C. Berendsen, J.P.M. Postma, W.F. van Gunsteren, A. DiNola, J.R. Haak, Molecular dynamics with coupling to an external bath, J. Chem. Phys. 81 (1984) 3684–3690.
[18] Schrödinger Suite 2009 Protein Preparation Wizard, Epik version 2.0, Schrödinger LLC., New York, NY, 2009; Impact version 5.5, Schrödinger LLC., New York, NY, 2009; Prime version 2.1, Schrödinger LLC., New York, NY, 2009.
[19] Maestro, version 9.0, Schrödinger Inc., New York, NY, 2009.
[20] Ligprep, version 2.3, Schrödinger Inc., New York, NY, 2009.
[21] Induced Fit Docking protocol; Glide version 5.5, Schrödinger LLC., New York, NY, 2011; Prime version 2.1, Schrödinger LLC., New York, NY, 2009.
[22] R.A. Friesner, J.L. Banks, R.B. Murphy, T.A. Halgren, J.J. Klicic, D.T. Mainz, M.P. Repasky, E.H. Knoll, M. Shelley, J.K. Perry, D.E. Shaw, P. Francis, P.S. Shenkin, Glide: a new approach for rapid, accurate docking and scoring. 1. Method and assessment of docking accuracy, J. Med. Chem. 47 (2004) 1739–1749.
[23] Schrodinger, LLC, The PyMOL Molecular Graphics System, version 1.3r1, 2010.
[24] A.C. Wallace, R.A. Laskowski, J.M. Thornton, LIGPLOT: a program to generate schematic diagrams of protein–ligand interactions, Protein Eng. 8 (1995) 127–134.
[25] PolarScreen™ Androgen Receptor Competitor Assay Kit, green protocol. <www.invitrogen.com>.
[26] R.J. Chen, T.Y. Chung, F.Y. Li, W.H. Yang, T.R. Jinn, J.T. Tzen, Steroid-like compounds in Chinese medicines promote blood circulation via inhibition of Na^+/K^+-ATPase, Acta Pharmacol. Sin. 31 (2010) 696–702.
[27] J.L. Zhang, H.Y. Tian, J. Li, L. Jin, C. Luo, W.C. Ye, R.W. Jiang, Steroids with inhibitory activity against the prostate cancer cells and chemical diversity of marine alga *Tydemania expeditionis*, Fitoterapia 83 (2012) 973–978.
[28] Y. Gong, Y. Li, Y. Lu, L. Li, H. Abdolmaleky, G.L. Blackburn, J.R. Zhou, Bioactive tanshinones in *Salvia miltiorrhiza* inhibit the growth of prostate cancer cells *in vitro* and in mice, Int. J. Cancer 129 (2011) 1042–1052.
[29] A.O. Brinkmann, L.J. Blok, P.E. de Ruiter, P. Doesburg, K. Steketee, C.A. Berrevoets, J. Trapman, Mechanisms of androgen receptor activation and function, J. Steroid Biochem. Mol. Biol. 69 (1999) 307–313.
[30] R. Jasuja, J. Ulloor, C.M. Yengo, K. Choong, A.Y. Istomin, D.R. Livesay, D.J. Jacobs, R.S. Swerdloff, J. Miksovska, R.W. Larsen, S. Bhasin, Kinetic and thermodynamic characterization of dihydrotestosterone-induced conformational perturbations in androgen receptor ligand-binding domain, Mol. Endocrinol. 23 (2009) 1231–1241.
[31] W.Q. Gao, Peptide antagonist of the androgen receptor, Curr. Pharm. Des. 16 (2010) 1106–1113.
[32] J. Richards, A.C. Lim, C.W. Hay, A.E. Taylor, A. Wingate, K. Nowakowska, C. Pezaro, S. Carreira, J. Goodall, W. Arlt, I.J. McEwan, J.S. de Bono, G. Attard, Interactions of abiraterone, eplerenone, and prednisolone with wild-type and mutant androgen receptor: a rationale for increasing abiraterone exposure or combining with MDV3100, Cancer Res. 72 (2012) 2176–2182.
[33] Q. Guo, J. Weng, X. Xu, M. Wang, X. Wang, X. Ye, W. Wang, M.A. Wang, Mutational analysis and molecular dynamics simulation of quinolone resistance proteins QnrA1 and QnrC from *Proteus mirabilis*, BMC Struct. Biol. 10 (2010) 33.
[34] C.B. Platania, S. Salomone, G.M. Leggio, F. Drago, C. Bucolo, Homology modeling of dopamine D2 and D3 receptors: molecular dynamics refinement and docking evaluation, PLoS One 7 (2012) e44316.
[35] C.E. Bohl, Z. Wu, D.D. Miller, C.E. Bell, J.T. Dalton, Crystal structure of the T877A human androgen receptor ligand-binding domain complexed to cyproterone acetate provides insight for ligand-induced conformational changes and structure-based drug design, J. Biol. Chem. 282 (2007) 13648–13655.
[36] J.S. Sack, K.F. Kish, C. Wang, R.M. Attar, S.E. Kiefer, Y. An, G.Y. Wu, J.E. Scheffler, M.E. Salvati, S.R.J. Krystek, R. Weinmann, H.M. Einspahr, Crystallographic structures of the ligand-binding domains of the androgen receptor and its T877A mutant complexed with the natural agonist dihydrotestosterone, Proc. Natl. Acad. Sci. USA 98 (2001) 4904–4909.
[37] Y. Kamano, Ring-opening reaction of 14,15-α,β-epoxide and 5,6-α,β-epoxide with hydroiodic acid, Chem. Pharm. Bull. 17 (1969) 1711–1719.
[38] G.L. Warren, C.W. Andrews, A.M. Capelli, B. Clarke, J. LaLonde, M.H. Lambert, M. Lindvall, N. Nevins, S.F. Semus, S. Senger, G. Tedesco, I.D. Wall, J.M. Woolven, C.E. Peishoff, M.S. Head, A critical assessment of docking programs and scoring functions, J. Med. Chem. 49 (2006) 5912–5931.
[39] I.A. Siddiqui, M. Asim, B.B. Hafeez, V.M. Adhami, R.S. Tarapore, H. Mukhtar, Green tea polyphenol EGCG blunts androgen receptor function in prostate cancer, FASEB J. 25 (2011) 1198–1207.
[40] Y.C. Yang, L.G. Meimetis, A.H. Tien, N.R. Mawji, G. Carr, J. Wang, R.J. Andersen, M.D. Sadar, Spongian diterpenoids inhibit androgen receptor activity, Mol. Cancer Ther. 12 (2013) 621–631.